

Impact of seawater carbonate chemistry on the calcification of marine bivalves

Jörn Thomsen^{*1,2}, Kristin Haynert^{1,3}, K. Mathias Wegner⁴, and Frank Melzner¹

¹Marine Ecology, GEOMAR Helmholtz Centre for Ocean Research, Kiel, Germany

²Marine Biology Research Division, Scripps Institution of Oceanography, University of California San Diego, La Jolla, CA 93092-0202, USA

³J.F. Blumenbach Institute for Zoology and Anthropology, Georg August University Göttingen, 37073 Göttingen, Germany

⁴Alfred Wegener Institute, Helmholtz Centre for Polar and Marine Research, Wadden Sea Station Sylt, D-25992 List, Germany

*corresponding author: jothomsen@ucsd.edu

Abstract

Bivalve calcification, particular of the early larval stages is highly sensitive to the change of ocean carbonate chemistry resulting from atmospheric CO₂ uptake. Earlier studies suggested that declining seawater [CO₃²⁻] and thereby lowered carbonate saturation affect shell production. However, disturbances of physiological processes such as acid-base regulation by adverse seawater pCO₂ and pH can affect calcification in a secondary fashion. In order to determine the exact carbonate system component by which growth and calcification are affected it is necessary to utilize more complex carbonate chemistry manipulations. As single factors, pCO₂ had no and [HCO₃⁻] and pH only limited effects on shell growth, while lowered [CO₃²⁻] strongly impacted calcification. Dissolved inorganic carbon (C_T) limiting conditions led to strong reductions in calcification, despite high [CO₃²⁻], indicating that [HCO₃⁻] rather than [CO₃²⁻] is the inorganic carbon source utilized for calcification by mytilid mussels. However, as the ratio [HCO₃⁻]/[H⁺] is linearly correlated with [CO₃²⁻] it is not possible to differentiate between these under natural seawater conditions. An equivalent of about 80 μmol kg⁻¹ [CO₃²⁻] is required to saturate inorganic carbon supply for calcification in bivalves. Below this threshold biomineralization rates rapidly decline. A comparison of literature data available for larvae and juvenile mussels and oysters originating from habitats differing substantially with respect to prevailing carbonate chemistry conditions revealed similar response curves. This suggests that the mechanisms which determine sensitivity of calcification in this group are highly conserved. The higher sensitivity of larval calcification seems to primarily result from the much higher relative calcification rates in early life stages. In order to reveal and understand the mechanisms that limit or facilitate adaptation to future ocean acidification, it is necessary to better understand the physiological processes and their underlying genetics that govern inorganic carbon assimilation for calcification.

1 Introduction:

The release of CO₂ by fossil fuel combustion and its subsequent absorption by the ocean has a fundamental impact on its carbonate chemistry. CO₂ uptake increases the dissolved inorganic carbon (C_T) in particular concentrations of seawater CO₂ (or partial pressure, pCO₂) and HCO₃⁻. These changes cause an acidification of the oceans and results in a decline of [CO₃²⁻]. Numerous studies demonstrated that ocean acidification interferes with the calcification process in many marine organisms (e.g. Kroeker, et al. 2010, Gazeau et al. 2014). It has been hypothesized that calcifiers are mainly impacted by the decline in [CO₃²⁻] and the corresponding decrease of the calcium carbonate saturation state Ω. Undersaturation (Ω<1) with respect to calcium carbonate is expected to cause dissolution of existing calcium carbonate structures or can impact shell formation directly (Miller et al. 2009, Thomsen et al. 2010, Rodolfo-Metalpa et al. 2011, Pansch et al. 2014).

However, whereas a large number of studies investigated the general response of calcifiers to ocean acidification, only few tried to disentangle the mechanistic response to specific carbonate chemistry species to test this hypothesis (Jury et al. 2010, Bach et al. 2011, de Putron et al. 2011, Suffrian et al. 2011, Waldbusser et al. 2011, Gazeau et al. 2012, Keul et al. 2013, Haynert et al. 2014, Waldbusser et al. 2014). In fact, studies performed with multicellular heterotrophs that do not compensate the ocean acidification induced decline in extracellular pH by means of HCO_3^- accumulation, revealed a strong correlation of calcification rate with ambient seawater $[\text{CO}_3^{2-}]$ and the directly related Ω . In contrast, calcification rate increased as a result of higher $[\text{CO}_3^{2-}]/\Omega$ in the extracellular/calcifying fluids in pHe regulating animals (Gutowska et al. 2010, Maneja et al. 2013). Although these findings match the general hypothesis of the sensitivity of calcifiers to ocean acidification it is unclear why seawater $[\text{CO}_3^{2-}]$ or Ω plays such an important role in the biominerization process in marine organisms (Bach 2015). $[\text{CO}_3^{2-}]$ only contributes less than 10 % to the oceanic C_T pool, whereas HCO_3^- contributes >90 %. Furthermore, its availability is highly variable due to the strong dependency on seawater pH and concentrations drastically decline at pH values below 8.5. Whereas the change in $[\text{CO}_3^{2-}]$ and the related change in saturation state Ω has been suggested to impact calcification directly (Gazeau et al. 2011, Waldbusser et al. 2014), reductions in seawater pH and increases in $p\text{CO}_2$ affect physiological processes such as acid-base regulation. It may thereby impact calcification in a secondary fashion via reductions in scope for growth (Melzner et al. 2013, Dorey et al. 2013).

The detailed mechanisms of calcification in bivalves are still not definitely elucidated and the hypotheses are controversial. Recently, the involvement of an amorphous calcium carbonate (ACC) precursor has been suggested which is produced in an intracellular compartment and subsequently exocytosed from the calcifying epithelia and transported to the site of shell formation (Mount et al. 2004, Weiner and Addadi 2011). The shell formation potentially involves the combined action of mantle epithelium and haemocytes which carry CaCO_3 to the site of shell formation (Mount et al. 2004, Johnstone et al. 2015). The precursor is then integrated into an organic matrix framework and remains either transiently in the amorphous state or crystallizes into a specific polymorph such as aragonite or calcite depending on the specific properties of matrix proteins (Weiss et al. 2002, Jacob et al. 2008). However, the presence of transient ACC has been only confirmed for larvae (Weiss et al. 2002) and adults of freshwater bivalves (Jacob et al. 2011) but still needs to be proven for marine bivalves in general. Nevertheless, for the production of CaCO_3 at either the shell margin or for intracellular ACC formation relatively large amounts of carbonate equivalents need to be accumulated in and transported across calcifying epithelia. This transport may potentially be accomplished by either uptake of seawater via endocytosis as suggested for foraminifera (Bentov et al. 2009) or direct $\text{HCO}_3^-/\text{CO}_3^{2-}$ carbonate transport across the cell membranes performed by a set of specific proteins and coupled to anion co-transport or cation exchange (Parker and Boron 2013). Independent of the exact mechanisms, calcification of bivalves in general and their larval stages in particular is especially sensitive to ocean acidification (Talmage and Gobler 2010, Barton et al. 2012, White et al. 2013, Gazeau et al. 2013).

Due to the high sensitivity of calcification to external seawater carbonate chemistry it is important to consider the environmental conditions the organism is exposed to. In open ocean habitats, $p\text{CO}_2$ and pH conditions are relatively stable (Hofmann et al. 2011). Furthermore, under fully saline conditions ($S = 32\text{-}37$) seawater titratable alkalinity (A_T) with its main components $[\text{HCO}_3^-]$ and $[\text{CO}_3^{2-}]$ is nearly linearly correlated with salinity, ranging between 2200 and 2400 $\mu\text{mol kg}^{-1}$ for most ocean regions (Millero et al. 1998). In contrast, much more variable carbonate chemistry ($p\text{CO}_2$, pH and A_T) is encountered in many coastal ecosystems and variability will increase even further in future (e.g. Hofmann et al. 2011, Cai et al. 2011, Melzner et al. 2013). In estuaries freshwater inputs lead to significantly lower salinity which generally reduces alkalinity (Miller et al. 2009). The Baltic Sea is an example of a brackish water habitat with eastward declining salinity and alkalinity due large freshwater inputs from the surrounding land masses. Although salinity decreases to almost 0, the high riverine A_T load causes relatively high A_T values that are significant higher than expected from dilution of seawater with distilled water (1200-1900 $\mu\text{mol kg}^{-1}$, Beldowski et al. 2010). Nevertheless,

due to the comparatively low A_T even small increases in atmospheric pCO_2 will cause low saturation or even undersaturation with respect to aragonite in the Baltic and estuaries in general (Miller et al. 2009, Waldbusser et al. 2011, Melzner et al. 2013). Coastal, brackish habitats might therefore be hotspots for bivalve vulnerability to future ocean acidification.

This study contributes to an understanding of the mechanisms and sensitivities of calcification in bivalves, with a focus on larval stages. For this purpose, experiments with strong modifications of the specific carbonate system parameters pCO_2 and A_T and meta-analyses of the calcification response of bivalves exposed to changes in carbonate chemistry have been conducted. We hypothesize that the calcification process in bivalves is highly dependent on external seawater carbonate chemistry and in particular on HCO_3^- availability as a substrate and favorable pH conditions.

2 Material and Methods:

2.1 Animal collection and maintenance

Adult and juvenile *Mytilus edulis* specimens were collected from 1 m depth in Kiel Fjord, Baltic Sea. For experiments with larvae, adults were transferred into a flow-through setup over night and spawning was induced the next day. For Exp. 4, parental animals were transferred to Sylt Dec 20th 2013, North Sea, and acclimated for 4 months to high salinities ($S=28.5 \text{ g kg}^{-1}$) in a net cage before they were transported back to Kiel prior to spawning (April 15th 2014). Juveniles were directly placed in the experimental units after measurement of initial length and wet mass. All experiments were conducted with four replicates per treatment in constant temperature rooms at GEOMAR in Kiel, Germany. Larvae or juveniles were placed in 500 mL experimental units which were aerated with humidified air with constant pCO_2 levels (see details below).

2.2 Experimental set up

2.2.1 Exp. 1: juvenile experiment

For the experiment on the calcification response of juvenile mussels, individuals with an initial mean shell length of $706 \pm 37 \mu\text{m}$ were collected on November 8th 2013 in Kiel Fjord and transferred to experimental units filled with 0.2 μm filtered seawater. The experiment lasted for three weeks and specimens were fed twice a day with a *Rhodomonas sp.* suspension resulting in initial concentrations of $25000 \text{ cells ml}^{-1}$. Algae were cultured in artificial seawater supplemented with Provasoli's enriched seawater (PES) in 7 L plastic bags under constant illumination and aeration (for details see Thomsen et al. 2010). The densities of algae cultures was measured daily using a particle counter (Coulter Counter, Beckmann GmbH, Germany) in order to calculate the volume which was needed to be added to reach desired densities in experimental units. Water was exchanged twice a week in order to avoid accumulation of waste products and significant influence of microbial activity and calcification on seawater alkalinity. The experiment was terminated by removing specimens from the experimental units after 21 days. Somatic tissues and shells were separated, dried at 60° C over night, shell lengths were measured by taking pictures using a stereo microscope (Leica F165, Leica Microsystems GmbH, Wetzlar, Germany) which were analyzed using ImageJ 1.43u. Shell mass was determined using a balance (Sartorius, Germany). Initial shell mass was calculated from a regression of measured shell length and shell mass (shell mass (mg) = $23.8 \times SL(\text{mm})^{2.75}$, $R^2=0.95$, $n=31$, shell length range 6-12 mm). Calcification was calculated by subtraction of the initial shell mass from final shell mass. The organic content of shells was not considered which leads to a minor overestimation of calcification rates (<10%, Thomsen et al. 2013). During the experiment, control mussel shell length and mass increased by a factor of 1.6 and 2.6, respectively.

2.2.2 Exp. 2+3+4: larval experiments

The experiments 2+3 were conducted in June 2012 (Exp. 2) and 2014 (Exp. 3) which is the main spawning season in the Baltic. Experiment 4 was conducted in April as animals were acclimated to North Sea temperatures which are higher. Adult individuals were placed in separate 800 ml beakers filled with 0.2 μm filtered seawater and gently aerated with pressurized air. Spawning was induced by rapidly increasing seawater temperature by 5° C above ambient temperate using heaters. Spawning usually started after 20 to 40 minutes following heat shock treatment. Egg densities were determined by counting three replicated sub samples using a stereomicroscope. Fertilization was carried out by additions of sperm solution pooled from three males to eggs from 3 females. Once the 4-8 cell stage was reached, embryos were transferred into the experimental units approximately 4 hours post fertilization at an initial density of 10 embryos ml^{-1} . Experimental duration of the larval experiment was restricted to the lecithotrophic phase and larvae were not fed. After the D-veliger stage was reached in all treatments (day 4), larval samples were taken and preserved with 4% paraformaldehyde and buffered using 10 mM NaHCO_3 .

2.3 Carbonate chemistry manipulation:

The dependency of juvenile and larval calcification on seawater carbonate chemistry speciation was determined by adjusting seawater alkalinity using 1M HCl and 1 M NaHCO_3 (for details see Table 1) and aeration with different $p\text{CO}_2$ levels (Exp. 1: 390 and 4000 μatm , Exp. 2: 390 and 2400 μatm , Exp. 3: 0 and 390 μatm , Exp. 4: 390 and 2400 μatm). $p\text{CO}_2$ treatments were realized using the central gas mixing facility of GEOMAR (390, 2400 and 4000 μatm), CO_2 free air was generated by using a soda lime CO_2 scrubber (Intersorb PlusTM, Intersurgical, Germany).

Carbonate chemistry was constrained by measuring seawater pH and either A_T in the juvenile (Exp. 1) or C_T in the larval experiment (Exp. 2+3) from discrete samples collected at the beginning and after termination of the experiment (Exp. 1-4) and weekly during the experiment (Exp. 1), respectively. Furthermore, pH_{NBS} was monitored in the experimental units daily (Exp. 2+3) or three times a week (Exp. 1). Analyses of A_T , C_T , and pH were performed immediately after sampling without poisoning. pH was determined either on NBS scale using a WTW 340i pH meter or on the total scale using seawater buffers mixed for a salinity of 15 and measured using a 626 Metrohm pH meter. A_T was determined with a 862 Compact Titrosampler (Metrohm, USA), C_T using an AIRICA C_T analyzer (Marianda, Germany). A_T and C_T , measurements were corrected using CRM (Dickson et al. 2003). Carbonate chemistry parameters were calculated using the CO2sys program. For calculations, the KHSO_4 dissociation constant (Dickson et al. 1990) and the carbonate system dissociation constants K1 and K2 (Mehrbach et al. 1973, refitted by Dickson and Millero 1987) were used.

2.4 Calculation of larval and juvenile *Mytilus* calcification and metabolic rates:

Calcification rates were calculated for ontogenetic stages ranging from the formation of the first larval D-shell to the juvenile stage two years after settlement. Larval calcification was calculated (1) assuming a total of 24 h required for D-shell formation and (2) for later veliger stages using a shell length and mass correlation for *M. edulis* larvae (Sprung 1984a) and the maximal increment of larval shell length during the planktonic phase under optimal feeding and temperature conditions (18°C, 11.8 $\mu\text{m day}^{-1}$, Sprung 1984a). Respiration rates of similar sized larval stages were calculated from the oxygen consumption rates published by Sprung (1984b, 18°C) and converted into $\text{nmol ind}^{-1} \text{h}^{-1}$. Other studies have obtained similar relationships for calcification (Jespersen and Olsen 1982) and respiration rate (Riisgård and Ranglov 1981) in the same species. Calcification rates of metamorphosed settled mussels were calculated from shell mass increments published for *M. edulis* kept under control $p\text{CO}_2$ (< 550 μatm) and optimized feeding conditions (Thomsen et al. 2010, Thomsen and Melzner 2010, Melzner et al. 2011, Thomsen et al. 2013) without considering the organic content of shell mass and its small ontogenetic change during the early benthic stage (Jørgensen 1976, Thomsen et al. 2013).

2.5 Meta-analysis of bivalve calcification in ocean acidification experiments

A meta-analysis was performed in order to compare the calcification performance of larvae and juveniles over a range of calculated seawater $[CO_3^{2-}]$. Published data including the measurements from this study were used. The increment of shell mass (juveniles) and D-shell length (larvae) was considered as a measure for calcification performance. For the analysis of larval calcification only data published for unfed lecithotrophic mytilid (*M. edulis*, *trossulus*, *galloprovincialis*, *californianus*), oyster (*Crassostrea gigas*, *Saccostrea glomerata*), scallop (*Pecten maximus*, *Argopecten irradians*) and clam larvae (*Macoma baltica*) were considered (Andersen et al. 2013, Barros et al. 2013, Frieder et al. 2014, Gazeau et al. 2010, 2011, Kurihara et al. 2007, 2009, Parker et al. 2010, Sunday et al. 2011, Timmins-Shiffman et al. 2012, Van Colen et al. 2012, Vitahkari et al. 2013, White et al. 2013, this study). In order to be able to compare the published data which differed in absolute sizes of larvae (potentially due to slightly differing experimental duration, temperatures, species size, maternal/paternal effects) and weight in juveniles (due to age), values are expressed as the relative calcification of a treatment compared to control conditions (=100%). This approach potentially masks a further increase of calcification at higher $[HCO_3^-]/[H^+]$. However, the plot of measured shell size data against seawater $[HCO_3^-]/[H^+]$ depicts that a shell length does not significantly increase at higher $[HCO_3^-]/[H^+]$ values and the response curve is similar to the meta-analysis (Fig. 4A, B, D). Calcification responses were not corrected for temperature differences between the studies as data represent the relative response under changed carbonate chemistry to an internal control. Carbonate chemistry parameters were either read from tables or recalculated from the provided data published in the manuscripts according to experimental temperature and salinity conditions using CO2sys and the settings described above (Table S1 and S2 in the supplement).

2.5 Statistics:

Data were analysed using ANOVA and Tukey Posthoc test following tests for normal distribution using Shapiro Wilks test with Statistica 8. If assumption for parametric testes were not given, non-parametric Kruskal-Wallis test was applied. Regression analyses were performed using Sigma Plot 10. Data points in graphs depict mean of replicates \pm standard deviation.

3 Results:

3.1 Impact of carbonate chemistry speciation on bivalve calcification

Calcification rates of juveniles *Mytilus edulis* (Exp. 1) kept under elevated pCO_2 (4000 μ atm) and control alkalinity were lower (17.7 ± 2.3 mg) in comparison to those obtained under control pCO_2 (27.0 ± 4.9 mg, Fig. 1). Reduction of alkalinity resulted in lowered shell growth under control pCO_2 (13.4 ± 1.1 mg) and increased alkalinity at high pCO_2 enabled higher calcification rates that were similar to those of control animals (28.6 ± 2.5). In Exp. 1, maximum shell mass growth of juveniles depended on seawater $[CO_3^{2-}]$ and was reduced at low concentrations (Table 2).

Depending on water temperature, formation of the first larval shell in *Mytilus* is completed after about 2 days whereby low temperature and adverse carbonate system conditions can cause a substantial delay (Sprung et al. 1984a, Supplement Fig. 2). In experiment 2 (pCO_2 : 390 and 2400 μ atm, control A_T : 1950 - 2000 μ mol kg^{-1}) larvae were sampled after four days in order to ensure fully developed PDI shells in all treatments. Larvae kept under low pCO_2 had a mean shell length of 117.4 ± 8.4 μ m when raised under control alkalinity conditions. In comparison, shell size decreased significantly to 92.3 ± 9.0 μ m in the treatment with elevated pCO_2 (Fig. 2). Lowering $[CO_3^{2-}]$ under control pCO_2 by means of HCl addition resulted in a similar decline of larval shell size. In contrast, high pCO_2 treatment and $NaHCO_3$ addition increased seawater $[CO_3^{2-}]$ and larval shell sizes were similar to animals from control pCO_2 and alkalinity. In summary, seawater $[CO_3^{2-}]$ had a significant effect on shell length (Table 2).

In Experiment 3 ($p\text{CO}_2$: 0 and 390 μatm) larvae were exposed to low C_T treatments by aeration with 0 μatm $p\text{CO}_2$ air and either control (low C_T 1) or reduced alkalinity (low C_T 2). The treatment with CO_2 free air increased seawater pH_{NBS} to 8.76 ± 0.06 (low C_T 1) and 8.61 ± 0.11 (low C_T 2) at A_T values of $1,471 \pm 75$ and $405 \pm 66 \mu\text{mol kg}^{-1}$, respectively and simultaneously decreased seawater C_T (Table 1). As a consequence, $[\text{HCO}_3^-]$ was reduced to $1,169 \pm 95$ and $342 \pm 67 \mu\text{mol kg}^{-1}$. However, due to the high seawater pH, $[\text{CO}_3^{2-}]$ remained relatively high at 300 ± 20 and $62 \pm 8 \mu\text{mol kg}^{-1}$. Shell length of larvae was greatest under control conditions ($111.9 \pm 6.8 \mu\text{m}$) and was significantly reduced in the low C_T treatments with $98.8 \pm 10.0 \mu\text{m}$ (low C_T 1) and $92.1 \pm 1.2 \mu\text{m}$ (low C_T 2, ANOVA, $F: 8.26$, $p<0.01$, Table 2). Plotting shell lengths against seawater $[\text{CO}_3^{2-}]$ revealed no correlation of calcification with $[\text{CO}_3^{2-}]$ when $[\text{HCO}_3^-]$ was low at the same time (Fig. 3).

In Exp. 4, larvae were exposed to a range of seawater $[\text{CO}_3^{2-}]$ (or $[\text{HCO}_3^-]/[\text{H}^+]$) values between 240 and $11 \mu\text{mol kg}^{-1}$ (Table 1). The obtained shell length data confirmed Exp. 2+3 as calcification rates were affected by low $[\text{CO}_3^{2-}]$. At the same time, it revealed that shell size at day 3 did not increase further at increased $[\text{CO}_3^{2-}]$ corresponding to an $\Omega_{\text{aragonite}}$ of up to 3.77, but remained fairly constant ($107.3 \pm 6.2 \mu\text{m}$, Fig. 4D). The response curve can be adequately described by an exponential rise to maximum or a power function (Supplementary Fig. S3).

3.2 Meta-analysis:

The comparison of published data on larval calcification revealed the strong correlation of shell size and seawater $[\text{HCO}_3^-]/[\text{H}^+]$ (Fig. 4A), $\Omega_{\text{aragonite}}$ (Fig. 4B), $[\text{CO}_3^{2-}]$ and C_T/H^+ (Supplementary Fig. 1 C-G). The overall response appears to be similar in all tested larval mytilid, oyster and clam species and can be described best by an exponential rise to maximum function (plotted against $[\text{HCO}_3^-]/[\text{H}^+]$: $(54.2 \pm 7.7) + 44.4 (\pm 7.1) \times (1 - e^{(-20 (\pm 4.1) \times [\text{CO}_3^{2-}])})$, $r^2 = 0.52$, $F = 50.0$, $p<0.01$). As the four parameters are almost linearly correlated to each other under similar temperature and salinity and realistic pH conditions, the calcification response appears to be similar. Calcification drastically declines below a critical threshold equivalent to a $[\text{HCO}_3^-]/[\text{H}^+]$ of 0.1, $\Omega_{\text{aragonite}}$ of 1 and $[\text{CO}_3^{2-}]$ of about $80 \mu\text{M}$, but appears to be relatively unaffected to changed carbonate system conditions at higher values (Fig. 4A,B, Supplementary Fig. C). In agreement with the data on larval calcification response, shell mass increment of juvenile, settled *M. edulis* followed a similar relationship (Fig. 4C). Regressions of relative calcification rates of both ontogenetic stages, larvae and juveniles, did not significantly differ from each other (ANCOVA, factor $[\text{HCO}_3^-]/[\text{H}^+]$, $F: 38.3$, $p<0.01$, factor ontogenetic stage $p\text{CO}_2$ $F: 2.62$, $p>0.05$, Table 2).

Absolute calcification rates of *M. edulis* increase during ontogeny from planktonic larval to benthic life stages from 0.01 to $958 \text{ nmol ind}^{-1} \text{ h}^{-1}$ (Fig. 5B). However, mass specific calcification rate (per mg drymass) was highest during D-shell formation with $767 \text{ nmol h}^{-1} \text{ mg}^{-1}$ and decreased with age to about $58.4 \text{ nmol h}^{-1} \text{ mg}^{-1}$ in juveniles (Fig. 5C). The high calcification rate during D-shell formation is also depicted in Fig 5A. During this period, calcification rate is much higher than during the next days and comparable rates are only reached at the end of the planktonic life phase (Fig. 5A). Calcification rates are compared with overall metabolic processes depicted as oxygen consumption rates. In contrast to calcification, individual based respiration rates are similar in trochophora and early shelled veliger, relatively lower than calcification during D-shell formation and steadily increase with biomass in growing larvae (Fig. 5A).

4 Discussion

The present study confirms the apparent correlation of shell formation and seawater $[\text{CO}_3^{2-}]$ or Ω in bivalves under conditions resembling natural seawater (Gazeau et al. 2011, Waldbusser et al. 2014). However, under C_T limiting conditions it becomes evident for the first time that HCO_3^- but not CO_3^{2-} is the substrate used for calcification. In our laboratory experiments, seawater $p\text{CO}_2$, pH and $[\text{HCO}_3^-]$ as

single factors did not or only to a small degree explained the observed decline in calcification rates. High $p\text{CO}_2$ causes acidification of intra- and extracellular fluids as $[\text{CO}_2]$ levels need to increase to the same extend in order to maintain a diffusion gradient between animal and ambient seawater. Low seawater pH causes higher passive proton leakage into the cytosol and thereby elevates costs for proton removal from the animal tissues by means of active transport (Boron et al. 2004). However, increased costs for regulation of intracellular acid-base homeostasis in somatic, non calcifying tissues seem to be of minor importance for the overall performance of these bivalve genera (see also Waldbusser et al. 2014). This speaks for a cost efficient acid-base regulation system in bivalves, which is potentially related to the fact that control of acid-base homeostasis is limited to the intracellular space. The pH of the much larger extracellular compartments, haemolymph and extrapallial fluid, remain unregulated and decline in acidified seawater (Thomsen et al. 2010, 2013, Heinemann et al. 2012). In contrast, a substantial fraction of the bivalve energy budget is dedicated to biomineralization processes, particularly the production of shell organic matrix (Palmer 1992, Thomsen et al. 2013, Waldbusser et al. 2013). Adverse conditions for calcification may then secondarily affect growth by reducing the energy available for protein biosynthesis (Stumpp et al. 2011, Dorey et al. 2013, Waldbusser et al. 2013, Pan et al. 2015). At the same time, growth is potentially slowed down secondarily by space limitation within the shell (Riisgård et al. 2014).

As long C_{T} is not limiting, the critical conditions of seawater carbonate chemistry for calcification are at a $[\text{HCO}_3^-]/[\text{H}^+]$ of 0.1 equivalent to a CO_3^{2-} concentration of about $80 \mu\text{mol kg}^{-1}$ or $\Omega_{\text{aragonite}}$ of about 1. Below this threshold calcification starts to decline strongly. On the other hand, higher $[\text{HCO}_3^-]/[\text{H}^+]$ does not lead to a further increase in calcification, which suggests a C_{T} saturation of the calcification mechanism. In particular at low alkalinity conditions, future levels of elevated CO_2 concentrations might have a substantial effect on calcification, whereas high alkaline water may potentially partially buffer negative effects (Miller et al. 2009, Fernandez-Reiriz et al. 2012, Thomsen et al. 2013). Nevertheless the result of the larval experiment conducted under C_{T} limiting conditions suggests that not the CO_3^{2-} concentration or the related Ω itself is determining calcification rates. Similar results were obtained for corals and the coccolithophore *Emiliana huxleyi* (Jury et al. 2010, Jokiel 2013, Bach 2015). Instead, calcification seems to depend on external HCO_3^- concentrations as calcification significantly declined at lowered $\text{HCO}_3^- (<1000 \mu\text{mol kg}^{-1})$ despite high $[\text{CO}_3^{2-}]$. This suggests that, most probably, HCO_3^- is the substrate used for calcification. Its availability in seawater is about 10 fold higher compared to CO_3^{2-} and its concentration does not significantly change within the naturally prevailing pH conditions observed in seawater (c.f. Bach 2015). Calcification requires a concentration mechanism for Ca^{2+} and CO_3^{2-} either in specialized membrane enclosed intracellular vesicles to produce the amorphous calcium carbonate (ACC) precursor or directly at the site of calcification (Weiner and Addadi 2011). Enrichment of HCO_3^- in the lumen of calcifying vesicles or the site of shell formation is likely performed via solute carrier (SLC) transporters of the families SCL4 and SLC26 such as $\text{Cl}^-/\text{HCO}_3^-$ exchangers (AE) or $\text{Na}^+/\text{HCO}_3^-$ co-transporters (NCBT, Parker and Boron 2013). A study carried out over a wide range of seawater $[\text{HCO}_3^-]$ confirmed its important role in the calcification process compared to $[\text{CO}_3^{2-}]$ (Jury et al. 2010). Reduced calcification under low seawater $C_{\text{T}}/\text{HCO}_3^-$ indicates that the velocity of C_{T} uptake is rate limited, independent of its mechanism: via endocytosis by vesicle formation or transmembrane ion transport proteins. Nevertheless, in a realistic ocean acidification scenario, seawater $[\text{HCO}_3^-]$ slightly increases due to elevated seawater C_{T} , but calcification rate in general declines. Therefore, the explanatory power of $[\text{HCO}_3^-]$ under natural conditions (e.g. $\text{HCO}_3^- > 1000 \mu\text{mol kg}^{-1}$) is low as HCO_3^- is not limiting and the dependency of calcification on its availability is barely visible. However, the conversion of bicarbonate into carbonate generates an equimolar number of protons at the site of CaCO_3 formation which need to be excreted from calcifying cells. The excretion along a proton gradient might be at least partly passive and may thereby only marginally impact the cellular energy budget when seawater conditions are suitable. Thus, lowered seawater pH diminishes the H^+ gradient between the calcifying epithelia and the ambient water which needs to be counterbalanced by up regulation of active H^+ extrusion mechanisms (Stumpp et al. 2012). If the regulatory capacities can not fully compensate for the adverse ambient conditions calcification rates remain reduced. Therefore, pH is a good predictor

of the calcification response under normal A_T conditions ($>2000 \mu\text{mol kg}^{-1}$, e.g. Frieder et al. 2014). In experiments with strong carbonate chemistry modifications, such as lowered A_T , the close correlation disappears as the reduced HCO_3^- availability is not considered. Therefore, the combination of both parameters, carbon availability and H^+ gradient, expressed as the ratio of seawater $[\text{HCO}_3^-]/[\text{H}^+]$ which is linearly correlated to $[\text{CO}_3^{2-}]$ and Ω predicts the calcification response best (Bach 2015). Whereas Ω needs to be supersaturated at the site of shell formation in order to facilitate crystal growth (Waldbusser et al. 2013), the reduction in calcification rate in marine organisms in response to reduced ambient $[\text{CO}_3^{2-}]$ and Ω is potentially a misinterpretation of the complex chemical speciation of the carbonate system. Consequently, one should probably rather speak of seawater ' $[\text{CO}_3^{2-}]$ equivalents' ($[\text{CO}_3^{2-}]_{\text{eq}}$). Under natural conditions, high seawater $[\text{CO}_3^{2-}]$ and Ω correspond to high HCO_3^- availability and relatively high pH of about 8, thus a large proton gradient between calcifying tissue and ambient seawater. These conditions provide enough HCO_3^- and enable fast extrusion of excess H^+ and are therefore beneficial for calcification.

Earlier studies suggested that the isolation of the shell formation site in early larvae is not as efficient as in later stages and therefore more sensitive to disturbances of the carbonate chemistry (Waldbusser et al. 2013). The results of our experiments, however, suggest that the ability of C_T accumulation and acid-base regulation in calcifying epithelia of mytilid bivalves do not seem to differ substantially between larval and benthic stages as the response to external carbonate chemistry is similar in both. Despite the fact that the calcifying organ changes during ontogeny: the first shell (prodissococonch I) is secreted by the shell gland and, subsequently, the shell field (Kniprath 1980, 1981). In later larval and juvenile stages, calcification is performed by the mantle tissue. Following settlement and metamorphosis, the mineralogy of the shell changes: while veliger prodissococonch I and II are exclusively composed of amorphous and aragonitic CaCO_3 (Medakovic 2000, Weiss et al. 2002, Weiss and Schönitzer 2006), the newly formed shell of juveniles consists of calcite, which is a more stable polymorph (Medakovic 1997). Nevertheless, this shift to a more stable polymorph does not seem to cause higher tolerance of the calcification process itself to adverse carbonate chemistry. It may, however, support the maintenance of calcified shells in undersaturated conditions in settled mussels. In fact, the higher sensitivity of larval calcification and PD I formation in particular seems to be primarily related to the much higher relative calcification rates per unit somatic body mass (Waldbusser et al. 2013, Fig. 5a+c). Thus, adverse carbonate system conditions have a much stronger effect in the early life stages. The response curve to ambient $[\text{CO}_3^{2-}]_{\text{eq}}$ obtained for bivalves in this study suggests that growth and development is not limited by calcification under high $[\text{CO}_3^{2-}]_{\text{eq}}$ conditions as calcification does not (Fig 4, Suppl. Fig. 3) or only slightly increases further (Waldbusser et al. 2014). At high $[\text{CO}_3^{2-}]_{\text{eq}}$, growth is potentially restricted by the rate of protein and carbohydrate synthesis for somatic tissue and the shell matrix production. This is supported by calculations of the larval energy budget: depending on the exact stoichiometry of H^+ transport, energetic costs for protein synthesis exceed those for acid-base regulation ($=\text{CaCO}_3$ formation) by a factor of three (Palmer 1992, Waldbusser et al. 2013). However, when environmental conditions are becoming more adverse calcification rates starting to slow down as (I) the kinetics of biomineralization are directly affected and cannot be compensated or (II) the scope for growth is reduced due to higher costs for ion regulation (Melzner et al. 2011, Waldbusser et al. 2013). At least juveniles are able to compensate for the adverse environment when food, thus energy, supply is abundant (Melzner et al. 2011, Thomsen et al. 2013) which suggests that reduced scope for growth is the main reason for lower calcification. Importantly, it has to be considered that biomineralization does not only require an increase of $[\text{CO}_3^{2-}]$, but at the same time is accompanied by a substantial reduction of the Mg^{2+} concentration in the shell compared to that of seawater (Lorens and Bender 1980). If this highly controlled reduction is an active, energy consuming process the related costs may exceed those of H^+ transport by far, as the molar number of ions required to be transported is much larger (Zeebe and Sanyal 2002). According to boron isotopes, mussels do not seem to increase the pH at the site of shell formation higher than ~ 7.5 which is sufficient for calcification as long as $[\text{Mg}^{2+}]$ are reduced in the calcifying fluid (Heinemann et al. 2012). Only the combination of both modifications enables the formation of CaCO_3 .

In relation to larval aerobic metabolic rates, calcification rates are especially high during the formation of PD I. This emphasizes the energetic importance of biomineralization in relation to all other vital processes at this life stage. Calcification rate strongly declines in relation to metabolism in the later planktonic phases (Sprung 1984b). The comparison of oxygen consumption rates with calcification rates also reveals that metabolic processes can not provide enough inorganic carbon for calcification – assuming a respiratory quotient of 0.7-1, i.e. generation of more or less equimolar amounts of CO_2 per O_2 respired. Therefore, larvae must take up seawater C_T which is also an energetically more efficient source of HCO_3^- than CO_2 , as only half of the protons are generated per mole of formed CaCO_3 . The high dependency of calcification on external C_T from the ambient seawater is further supported by isotopic data which revealed only a minor fraction of metabolic CO_2 (5-15%) but a large seawater signal in the shells of bivalves (McConaughey and Gillikin 2008, Waldbusser et al. 2013). The exact fraction of metabolic carbon in the shell differs in e.g. early and later larval shells (Waldbusser et al. 2013). This difference is potentially a result from passive diffusion of metabolic CO_2 to the site of CaCO_3 formation thereby increasing the fraction of metabolic carbon. Therefore the fraction depends on the ratio $C_{\text{calcified}} / C_{\text{respired}}$ which differs substantially during ontogeny, but may not necessarily indicate the degree of isolation from seawater.

As a consequence of detrimental changes in seawater carbonate chemistry, costs for calcification are increased and more energy is required to produce a similar amount of calcium carbonate when compared to control conditions. This is of particular importance, as the formation of the first shell is exclusively fueled by the energy reserves provided by the egg as the larvae can start feeding only after they have reached the shelled veliger stage after ca 2-3 days post fertilization (Waller 1980, Widdows 1991). The energy supply from the egg yolk enables maximal calcification rates and allows the early larvae to develop the D-shell independent of the food concentrations of the ambient environment (Moran and Manahan 2004). Once the first shell is produced, feeding larvae continue to calcify prodissoconch II but cease to grow if no food is available. The small remaining egg reserves and uptake of dissolved organic matter (DOM) from the ambient seawater may enable them to endure a short starvation period (Moran and Manahan 2004). Starvation in the first days of the larval period does not induce high mortality during the subsequent days but eventually affects final settlement success (His and Seaman 1992, Moran and Manahan 2004). The negative impact of low $[\text{CO}_3^{2-}]_{\text{eq}}$ on early larval development and final settlement success has been observed in field studies (Barton et al. 2012), although successful and abundant settlement has been observed under similar conditions as well (Thomsen et al. 2010). It has been suggested that the strong impairment of the larval energy budget under CO_2 stress might lead to an earlier depletion of their endogenous energy reserves which might eventually impact survival (Waldbusser et al. 2013). As low food concentrations limit larval growth, compensatory effects of higher food availability may play an important role in the planktonic phase similar to results reported for the benthic life phase (Sprung 1984a, Melzner et al. 2011, Thomsen et al. 2013). A recent study did not confirm this hypothesis for larvae of the oyster *Ostrea lurida*. Here, as a consequence of the limited larval clearance capacities, animals were potentially not limited by the provided food concentrations and growth rates leveled off in all treatments (Riisgård et al 1980, Hettinger et al. 2013).

In conclusion, the meta-analysis of juvenile mussels and larval calcification of mytilid mussels, oysters, scallops and clams revealed a similar response to lowered $[\text{HCO}_3^-]/[\text{H}^+]$ or $[\text{CO}_3^{2-}]_e$ in different species and populations. The limitation of biomineralization due to kinetic constraints in the calcifying fluid during shell formation have been suggested to cause the sensitivity of shell formation in larval bivalves (Waldbusser et al. 2013) which has been confirmed by this study. However, this study does not confirm the importance of $[\text{CO}_3^{2-}]$ or Ω in the ambient seawater (Waldbusser et al. 2014) or mechanistic differences between larval and juveniles stages. The results obtained under low seawater C_T , emphasizes the importance of a $[\text{HCO}_3^-]/[\text{H}^+]$ ratio for bivalve calcification which is linearly correlated to $[\text{CO}_3^{2-}]$ and Ω under the same temperature and salinity. This concept considers physiological constraints of acid-base regulation and the impact on the energy budgets of bivalves and is in accordance with principles of biomineralization obtained in other aquatic organisms as well

(Jokiel et al. 2013, Bach 2015). The mechanistic limitations of calcification in marine bivalves may potentially represent a barrier to rapid evolutionary adaptation to abiotic conditions expected for the future ocean. Therefore, more research is needed to understand the physiological basis of bivalve biomineralization machinery and its adaptability to adverse carbonate chemistry.

Authors contribution

J. T. designed the study, J. T. and K. H. conducted the experiments, meta-analyses and analyzed the data, K. M. W. supported the experimental work, J. T. and F. M. wrote the manuscript with support of all co-authors.

Acknowledgements

The authors thank Ulrike Panknin for supporting experiments and Florian Weinberger for providing soda lime. Further, Lennart Bach is acknowledged for helpful discussions. This study received funding from the BMBF project BIOACID subproject 3.4.

References

Andersen, S., Grefsrud, E. S., and Harboe, T.: Effect of increased $p\text{CO}_2$ level on early shell development in great scallop (*Pecten maximus* Lamarck) larvae, *Biogeosciences*, 10, 6161-6184, 2013.

Bach, L. T.: Reconsidering the role of carbonate ion concentration in calcification by marine organisms, *Biogeosci. Discuss.* 12, 6689-6722, 2015.

Bach, L. T., Riebesell, U., and Schulz, K. G.: Distinguishing between the effects of ocean acidification and ocean carbonation in the coccolithophore *Emiliania huxleyi*, *Limnol. Oceanogr.*, 56, 2040–2050, 2011.

Barton, A., Hales, B., Waldbusser, G., Langdon, C., and Feely, R.: The Pacific oyster, *Crassostrea gigas*, shows negative correlation to naturally elevated carbon dioxide levels: Implications for near-term ocean acidification effects, *Limn. Oceanogr.*, 57, 696-710, 2012.

Beldowski, J., Löffler, A., and Joensuu, L.: Distribution and biogeochemical control of total CO_2 and total alkalinity in the Baltic Sea, *J. Marine. Syst.*, 81, 252–259, 2010.

Bentov, S., Brownlee, C., and Erez, J.: The role of seawater endocytosis in the biomineralization process in calcareous foraminifera, *P. of the Natl. Acad. Sci. USA*, 106, 21500-21504, 2009.

Boron, W. F.: Regulation of intracellular pH, *Adv. Physiol. Educ.*, 28, 160-179, 2004.

Cai, W. J., Hu, X., Huang, W. J., Murrell, M. C., Lehrter, J. C., Lohrenz, S. E., Chou, W. C., Zhai, W., Hollibaugh, J. T., Wang, Y., Zhao, P., Guo, X., Gundersen, K., Dai, M., and Gong, G.C.: Acidification of subsurface coastal waters enhanced by eutrophication, *Nat. Geosci.*, 4, 766-770, 2011.

de Putron, S. J., McCorkle, D. C., Cohen, A. L., and Dillon, A. B.: The impact of seawater saturation state and bicarbonate ion concentration on calcification by new recruits of two Atlantic corals, *Coral Reefs*, 30, 321–328, 2011.

Dickson, A. G., and Millero, F. J.: A comparison of the equilibrium constants for the dissociation of carbonic-acid in seawater media, *Deep-Sea Res.*, 34, 1733–1743, 1987.

Dickson, A. G.: Standard potential of the reaction – $\text{AgCl} + \frac{1}{2} \text{H}_2 = \text{AgS} + \text{HClAq}$ and the standard acidity constant of the ion HSO_4^- – in synthetic sea-water from 273.15-K to 318.15-K, *J. Chem. Thermodyn.*, 22, 113–127, 1990.

Dickson, A. G., Afgan, J. D., and Anderson, G. C.: Reference materials for oceanic CO_2 analysis: a method for the certification of total alkalinity, *Mar. Chem.*, 80, 185–197, 2003.

Dorey, N., Lancon, P., Thorndyke, M., and Dupont, S.: Assessing physiological tipping point of sea urchin larvae exposed to a broad range of pH, *Glob. Change Biol.*, 19, 3355–3367, 2013.

Fernández-Reiriz, M. J., Range, P., Álvarez-Salgado, X. A., Espinosa, J., Labarta, U.: Tolerance of juvenile *Mytilus galloprovincialis* to experimental seawater acidification, *Mar. Ecol.-Prog. Ser.*, 454, 65–74, 2012.

Frieder, C. A., Gonzales, J. P., Bockmon, E. E., Navarro, M. O., and Levin, L.A.: Can variable pH and low oxygen moderate ocean acidification outcomes for mussel larvae, *Glob. Change Biol.*, 20, 754–764, 2014.

Gazeau, F., Gattuso, J. P., Dawber, C., Pronker, A. E., Peene, F., Peene, J., Heip, C. H. R., and Middelburg, J. J.: Effect of ocean acidification on the early life stages of the blue mussel *Mytilus edulis*, *Biogeosciences*, 7, 2051–2060, 2010.

Gazeau, F., Gattuso J. P., Greaves, M., Elderfield, H., Peene, J., Heip, C. H. R., and Middelburg, J. J.: Effect of carbonate chemistry alteration on the early embryonic development of the Pacific oyster (*Crassostrea gigas*), *PLOS ONE*, 6, e23010, 2011.

Gazeau, F., Parker, L. M., Comeau, S., Gattuso, J. P., O'Connor, W.A., Martin, S., Pörtner, H. O., and Ross, P. M.: Impacts of ocean acidification on marine shelled molluscs, *Mar. Biol.*, 160, 2207–2245, 2013.

Gutowska, M. A., Melzner, F., Pörtner, H. O., and Meier, S.: Cuttlebone calcification increases during exposure to elevated seawater pCO_2 in the cephalopod *Sepia officinalis*, *Mar. Biol.*, 157, 1653–1663, 2010.

Haynert, K., Schönfeld, J., Schiebel, R., Wilson, B., and Thomsen, J.: Response of benthic foraminifera to ocean acidification in their natural sediment environment: a long-term culturing experiment, *Biogeosciences*, 11, 1581–1597, 2014.

Heinemann, A., Fietzke, J., Melzner, F., Böhm, F., Thomsen, J., Garbe-Schönberg, D. Eisenhauer, A.: Conditions of *Mytilus edulis* extracellular body fluids and shell composition in a pH-treatment experiment: Acid-base status, trace elements and $\delta^{11}\text{B}$, 13, Q01005, 2012.

Hettinger, A., Sanford, E., Hill, T. M., Hosfelt, J.D., Russell, A. D., and Gaylord, B.: The influence of food supply on the response of Olympia oyster larvae to ocean acidification, *Biogeosciences*, 10, 6629–6638, 2013.

His, E., and Seaman, M. N. L.: Effects of temporary starvation on survival, and on subsequent feeding and growth, of oyster (*Crassostrea gigas*) larvae, *Mar. Biol.*, 114, 277–279, 1992.

Hofmann G. E., Smith J. E, Johnson K. S., Send, U., Levin, L. A., Micheli, F., Price, N. N., Peterson, B., Takeshita, Y., Matson, P.G., Crook, E. D., Kroeker, K., Gambi, M. C., Rivest, E. B., Frieder, C. A., Yu, P. C., and Martz, T. R.: High-Frequency Dynamics of Ocean pH: A Multi-Ecosystem Comparison, *PLOS ONE*, 6, e28983, 2011.

Jacob, D. E., Soldati, A. L., Wirth, R., Huth, J., Wehrmeister, U., and Hofmeister, W.: Nanostructure, composition and mechanisms of bivalve shell growth, *Geochim. Cosmochim. Ac.*, 72, 5401–5415, 2008.

Jacob, D. E., Wirth, R., Soldati, A. L., Wehrmeister, U., and Schreiber, A.: Amorphous calcium carbonate in the shells of adult *Unionoida*, *J. Struct. Biol.*, 173, 241-249, 2011.

Jespersen, H., and Olsen, K.: Bioenergetics of veliger larvae of *Mytilus edulis* L., *Ophelia*, 21 101-113. 1982.

Johnstone, M. B., Gohad, N. V., Falwell, E. P., Hansen, D. C., Hansen, K. M., and Mount, A. S.,: Cellular orchestrated biomineralization of crystalline composites on implant surfaces by the eastern oyster, *Crassostrea virginica* (Gmelin, 1791), *J. Exp. Mar. Biol. Ecol.*, 463, 8-16, 2015.

Jokiel, P. L.: Coral reef calcification: carbonate, bicarbonate and proton flux under conditions of increasing ocean acidification, *Proc. Roy. Soc. B*, 280, 20130031, 2013.

Jørgensen, C.: Growth efficiencies and factors controlling size in some mytilid bivalves, especially *Mytilus edulis* L.: review and interpretation, *Ophelia*, 15, 175–192, 1976.

Jury, C. P., Whitehead, R. F., and Szmant, A. M.: Effects of variations in carbonate chemistry on the calcification rates of *Madracis auretenra* (= *Madracis mirabilis* sensu Wells, 1973): bicarbonate concentrations best predict calcification rates, *Glob. Change Biol.*, 16, 1632–1644, 2010.

Keul, N., Langer, G., de Nooijer, L. J., and Bijma, J.: Effect of ocean acidification on the benthic foraminifera *Ammonia* sp. is caused by a decrease in carbonate ion concentration, *Biogeosciences*, 10, 6185–6198, 2013.

Kniprath, E.: Larval development of the shell and the shell gland in *Mytilus* (Bivalvia), *Roux Arch. Dev. Biol.*, 188, 201-204, 1980.

Kniprath, E.: Ontogeny of the molluscan shell field: a Review. *Zool. Scr.*, 10, 61-79, 1981.

Kroeker, K. J., Kordas, R. L., Crim, R. N., and Singh, G. G.: Meta-analysis reveals negative yet variable effects of ocean acidification on marine organisms, *Ecol. Lett.*, 13, 1419–1434, 2010.

Kurihara, H., Kato, S., and Ishimatsu A.: Effects of increased seawater $p\text{CO}_2$ on early development of the oyster *Crassostrea gigas*, *Aquat. Biol.*, 1: 91–98, 2007.

Kurihara, H., Asai, T., Kato, S., and Ishimatsu A.: Effects of elevated $p\text{CO}_2$ on early development in the mussel *Mytilus galloprovincialis*, *Aquat. Biol.*, 4: 225–233, 2008.

Lorens, R., B., and Bender, M. L.: The impact of solution chemistry on *Mytilus edulis* calcite and aragonite, *Geochim. Cosmochim. Ac.*, 44, 1265-1278, 1980.

Maneja, R. H., Frommel, A. Y., Geffen, A. J., Folkvord, A., Piatkowski, U., Chang, M. Y., and Clemmesen, C.: Effects of ocean acidification on the calcification of otoliths of larval Atlantic cod *Gadus morhua*, *Mar. Ecol.-Prog. Ser.*, 477, 251–258, 2013.

McConaughey T. A. and Gillikin, D. P.: Carbon isotopes in mollusk shell carbonates, *Geo. Mar. Lett.*, 28, 287–299, 2008.

Medakovic, D., Popovic, S., Gržetić, B., Plazonic, M., Hrs-Brenko, M.: X-ray diffraction study of calcification processes in embryos and larvae of the brooding oyster *Ostrea edulis*, *Mar. Biol.*, 129, 615-623, 1997.

Medakovic, D.: Carbonic anhydrase activity and biomineralization process in embryos, larvae and adult blue mussels *Mytilus edulis* L., *Helgol. Mar. Res.*, 54, 1–6, 2000.

Mehrback, C., Culberso, C. H., Hawley, J. E., and Pytkowic, R. M.: Measurement of apparent dissociation-constants of carbonic acid in seawater at atmospheric-pressure, *Limnol. Oceanogr.*, 18, 897–907, 1973.

Melzner, F., Stange, P., Trübenbach, K., Thomsen, J., Casties, I., Panknin, U., Gorb, S., Gutowska, M. A.: Food supply and seawater $p\text{CO}_2$ impact calcification and internal shell dissolution in the Blue Mussel *Mytilus edulis*, *PLOS ONE*, 6, e24223, 2011.

Melzner, F., Thomsen, J., Koeve, W., Oschlies, A., Gutowska, M.A., Bange, H. W., Hansen, H. P., and Körtzinger, A.: Future ocean acidification will be amplified by hypoxia in coastal habitats, *Mar. Biol.* 160, 1875–1888, 2013.

Miller, A. W., Reynolds, A.C., Sobrino, C., Riedel, G. F.: Shellfish face uncertain future in high CO_2 world: Influence of acidification on oyster larvae calcification and growth in estuaries, *PLOS ONE*, 4, e5661, 2009.

Millero, F. J., Lee, K., and Roch, M.: Distribution of alkalinity in the surface waters of the major oceans, *Mar. Chem.*, 60, 111–130, 1998.

Moran, A. L. and Manahan, D. T.: Physiological recovery from prolonged ‘starvation’ in larvae of the Pacific oyster *Crassostrea gigas*, *J. Exp. Mar. Biol. Ecol.*, 306, 17–36, 2004.

Mount, A. S., Wheeler, A. P., Paradkar, R. P., and Snider, D.: Hemocyte-mediated shell mineralization in the eastern oyster, *Science*, 304, 297–300, 2004.

Palmer, A. R.: Calcification in marine mollusks – how costly is it, *P. of the Natl. Acad. Sci. USA*, 89, 1379–1382, 1992.

Pansch, C., Schaub, I., Havenhand, J., and Wahl, M.: Habitat traits and food availability determine the response of marine invertebrates to ocean acidification, *Glob. Change Biol.*, 20, 765–777, 2014.

Parker, M. D. and Boron, W. F.: The divergence, actions, roles, and relatives of sodium-coupled bicarbonate transporters, *Physiol. Rev.*, 93, 803–959, 2013.

Riisgård, H. U., Randløv, A., Hamburger, K.: Oxygen consumption and clearance as a function of size in *Mytilus edulis* L. veliger larvae, *Ophelia*, 20, 179–183, 1981.

Riisgård, H. U., Larsen, P. S., Turja, R., and Lundgren, K.: Dwarfism of blue mussels in the low saline Baltic Sea – growth to the lower salinity limit, *Mar. Ecol.-Prog. Ser.*, 517, 181–192, 2014.

Rodolfo-Metalpa, R., Houlbrèque, F., Tambutté, É., Boisson, F., Baggini, C., Patti, F. P., Jeffree, R., Fine, M., Foggo, A., Gattuso, J. P., and Hall-Spencer, J. M.: Coral and mollusc resistance to ocean acidification adversely affected by warming, *Nat. Clim. Chang.*, 1, 308–312, 2011.

Sprung, M.: Physiological energetics of mussel larvae (*Mytilus edulis*), I. Shell growth and biomass, *Mar. Ecol.-Prog. Ser.*, 17, 283–293, 1984a.

Sprung, M.: Physiological energetics of mussel larvae (*Mytilus edulis*), III. Respiration, *Mar. Ecol.-Prog. Ser.*, 18, 171–178, 1984b.

Stumpp, M., Hu, M. Y., Melzner, F., Gutowska, M. A., Dorey, N., Himmerkus, N., Holtmann, W. C., Dupont, S. T., Thorndyke, M. C., and Bleich, M.: Acidified seawater impacts sea urchin larvae pH regulatory system relevant for calcification, *P. of the Natl. Acad. Sci. USA*, 109, 18192-18197, 2012.

Suffrian, K., Schulz, K. G., Gutowska, M. A., Riebesell, U., and Bleich, : Cellular pH measurements in *Emiliania huxleyi* reveal pronounced membrane proton permeability, *New Phytol.*, 190, 595–608, 2011.

Sunday, J. M., Crim, R. N., Harley, C. D. G., Hart, M. W.: Quantifying rates of evolutionary adaptation in response to ocean acidification, *PLOS ONE*, 6, e22881, 2011.

Talmage, S. C., and Gobler, C. J.: Effects of past, present, and future ocean carbon dioxide concentrations on the growth and survival of larval shellfish, *P. of the Natl. Acad. Sci. USA*, 107, 40, 17246-17251, 2010.

Thomsen, J., and Melzner, F.: Moderate seawater acidification does not elicit long-term metabolic depression in the blue mussel *Mytilus edulis*, *Mar. Biol.*, 157, 2667–2676, 2010.

Thomsen, J., Gutowska, M. A., Saphörster, J., Heinemann, A., Trübenbach, K., Fietzke, J., Hiebenthal, C., Eisenhauer, A., Körtzinger, A., Wahl, M., and Melzner, F.: Calcifying invertebrates succeed in a naturally CO₂-rich coastal habitat but are threatened by high levels of future acidification, *Biogeosciences*, 7, 3879–3891, 2010.

Thomsen, J., Casties, I., Pansch, C., Körtzinger, A., and Melzner, F.: Food availability outweighs ocean acidification effects in juvenile *Mytilus edulis*: laboratory and field experiments, *Glob. Change Biol.*, 19, 1017–1027, 2013.

Timmins-Schiffman, E., O'Donnell, M. J., Friedmann, C. S., and Roberts, S. B.: Elevated pCO₂ causes developmental delay in early larval Pacific oysters, *Crassostrea gigas*, *Mar. Biol.*, 160, 1973-1982, 2013.

Van Colen, C., Debusschere, E., Braeckman, U. Van Gansbeke, D., and Vincx, M.: The early life history of the clam *Macoma balthica* in a high CO₂ world, *PLOS ONE*, 7, e4655, 2012

Vihtakari, M., Hendriks, I. E., Holding, J., Renaud, P. E., Duarte, C. M., and Havenhand, J.N.: Effects of ocean acidification and warming on sperm activity and early life stages of the Mediterranean mussel (*Mytilus galloprovincialis*), *Water*, 5, 1890-1915, 2013.

Waldbusser, G. G., Voigt, E. P., Bergschneider, H., Green, M. A., and Newell, R. I. E.: Biocalcification in the eastern oyster (*Crassostrea virginica*) in relation to long-term trends in Chesapeake Bay pH, *Estuaries Coasts.*, 34, 221-231, 2011.

Waldbusser, G. G., Brunner, E. L., Haley, B. A., Hales, B., Langdon, C. J., and Prahl, F. G.: A developmental and energetic basis linking larval oyster shell formation to acidification sensitivity, *Geophys. Res. Lett.*, 40, 1–6, 2013.

Waldbusser, G. G., Hales, B., Langdon, C. J., Haley, B. A., Schrader, P., Brunner, E. L., Gray, M. W., Miller, C. A., and Gimenez, I.: Saturation-state sensitivity of marine bivalve larvae to ocean acidification, *Nat. Clim. Chang.*, 5, 273-280, 2014.

Waller, T. R.: Functional morphology and development of veliger larvae of the European Oyster, *Ostrea edulis* Linne, *Smithson. Contr. Zool.*, 328, 1-70, 1981

Weiner, S., and Addadi, L.: Crystallization pathways in biomineralization, *Annu. Rev. Mater. Res.*, 41, 21–40, 2011.

White, M. M., McCorkle, D. C., Mullineaux, L. S., and Cohen, A. L. Early exposure of bay scallops (*Argopecten irradians*) to high CO₂ causes a decrease in larval shell growth, PLOS ONE, 8, e61065, 2013.

Weiss, I. M., Tuross, N., Addadi, L., and Weiner, S.: Mollusc larval shell formation: Amorphous calcium carbonate is a precursor phase for aragonite, J. Exp. Zool., 293, 478-491, 2002.

Weiss, I. M., and Schönitzer, V., The distribution of chitin in larval shells of the bivalve mollusk *Mytilus galloprovincialis*, J. Struct. Biol., 153, 264-277, 2006.

Widdows, J.: Physiological ecology of mussel larvae, Aquaculture, 94, 147-163, 1991.

Zeebe, R. E., and Sanyal, A.: Comparison of two potential strategies of planktonic foraminifera for house building: Mg²⁺ or H⁺ removal? Geochim. Cosmochim. Ac., 66, 1159-1169, 2002.

Table 1. Carbonate chemistry parameters of the four experiments (mean \pm sd) calculated from measured C_T (larval experiments) or A_T (juvenile experiment) and pH (NBS or total scale)

experiment	salinity	temperature	treatment	A_T	C_T	pH	pCO_2	HCO_3^-	CO_3^{2-}	$[HCO_3^-]/[H^+]$
	g kg ⁻¹	°C	pCO_2/CO_3^{2-}	[μmol kg ⁻¹]	[μmol kg ⁻¹]	total scale	[μatm]	[μmol kg ⁻¹]	[μmol kg ⁻¹]	[mol]/[μmol]
Exp. 1 Juveniles	17.7 \pm 1.3	17.3 \pm 1.2	390/75	1976 \pm 87	1886 \pm 76	8.13 \pm 0.03	501 \pm 1	1784 \pm 68	83 \pm 11	0.24 \pm 0.02
			4000/12	2052 \pm 28	2104 \pm 199	7.65 \pm 0.58	5214 \pm 81	1935 \pm 132	10 \pm 0	0.04 \pm 0.01
			390/12	851 \pm 34	847 \pm 30	7.74 \pm 0.08	564 \pm 101	810 \pm 29	15 \pm 2	0.02 \pm 0.00
			4000/75	5765 \pm 74	5909 \pm 58	7.57 \pm 0.01	5649 \pm 99	5613 \pm 61	71 \pm 7	0.21 \pm 0.02
Exp. 2 Larvae	13.6 \pm 0.1	17.7 \pm 0.1	390/78	1943 \pm 17	1863 \pm 23	7.99 \pm 0.04	510 \pm 49	1766 \pm 27	78 \pm 6	0.17 \pm 0.01
			2400/20	1998 \pm 43	2032 \pm 41	7.49 \pm 0.04	1778 \pm 149	1936 \pm 40	27 \pm 3	0.03 \pm 0.01
			390/20	852 \pm 11	848 \pm 6	7.63 \pm 0.07	544 \pm 78	811 \pm 6	16 \pm 3	0.06 \pm 0.01
			2400/78	3418 \pm 133	3398 \pm 111	7.72 \pm 0.06	1775 \pm 207	3252 \pm 104	77 \pm 15	0.17 \pm 0.03

Exp. 3 Larvae	15.2 ± 0.2	16.0 ± 0.1	390/100	2056 ± 4	1942 ± 5	8.09 ± 0.01	404 ± 14	1825 ± 7	100 ± 3	0.23 ± 0.01
			0/300	1859 ± 47	1471 ± 75	8.76 ± 0.06	56 ± 13	1169 ± 95	300 ± 20	0.68 ± 0.05
			0/60	540 ± 57	405 ± 66	8.61 ± 0.11	24 ± 11	342 ± 67	62 ± 8	0.14 ± 0.02
Exp. 4 Larvae	28.5 ± 0.1	15.3 ± 0.2	390/235	3136 ± 2	2840 ± 2	8.15 ± 0.00	435 ± 1	2584 ± 2	240 ± 0	0.37 ± 0.00
			390/172	2659 ± 37	2863 ± 0	8.04 ± 0.07	508 ± 86	2284 ± 22	159 ± 25	0.25 ± 0.04
			390/116	1928 ± 309	1786 ± 270	7.99 ± 0.01	411 ± 75	1665 ± 279	106 ± 16	0.16 ± 0.02
			390/70	1457 ± 326	1361 ± 314	7.91 ± 0.00	382 ± 88	1279 ± 295	67 ± 16	0.10 ± 0.02
			390/32	1155 ± 7	1098 ± 5	7.77 ± 0.01	425 ± 4	1042 ± 4	40 ± 1	0.06 ± 0.00
			390/9	732 ± 46	712 ± 42	7.56 ± 0.04	451 ± 10	678 ± 40	16 ± 2	0.02 ± 0.00
			2400/235	6354 ± 59	6240 ± 61	7.70 ± 0.01	2850 ± 73	5938 ± 597	194 ± 0	0.30 ± 0.00
			2400/172	5558 ± 68	5474 ± 73	7.67 ± 0.01	2680 ± 72	5213 ± 71	159 ± 1	0.24 ± 0.00
			2400/116	4582 ± 42	4562 ± 38	7.57 ± 0.01	2814 ± 22	4350 ± 37	105 ± 3	0.16 ± 0.00
			2400/70	3527 ± 7	3571 ± 25	7.42 ± 0.04	3078 ± 313	3395 ± 18	58 ± 5	0.09 ± 0.01
			2400/32	2504 ± 42	2568 ± 41	7.31 ± 0.01	2857 ± 4	2427 ± 40	32 ± 1	0.05 ± 0.00
			2400/9	1393 ± 20	1479 ± 15	7.08 ± 0.02	2733 ± 102	1364 ± 18	11 ± 1	0.02 ± 0.00

Table 2. Statistic: ANOVA, Kruskal-Wallis and ANCOVA of calcification rates against seawater $[\text{CO}_3^{2-}]$ and $[\text{HCO}_3^-]/[\text{H}^+]$, significant results in bold

Experiment 1 +2					
ANOVA	SS	d.f.	MS	F	p
Exp. 1 juveniles	639	3	213	23.4	<0.01
Exp. 2 larvae	2301	3	767	11.8	<0.01
Experiment 3					
Kruskal-Wallis	group	d.f.	n	sum of ranks	
H: 6.61	p: < 0.05	390/100	2	4	40
		0/300		4	24
		0/60		4	14
Metanalysis juvenile and larval calcification, ANCOVA					
ANCOVA	SS	d.f.	MS	F	p
$[\text{HCO}_3^-]/[\text{H}^+]$	0.157	1	0.157	38.3	<0.01
ontog. stage	0.11	1	0.11	2.6	>0.05

Fig. 1. Exp. 1 Calcification response (measured as shell mass growth) of *M. edulis* juveniles kept under modified conditions for 15 days. Shell mass growth is plotted against seawater (A) $p\text{CO}_2$, (B) $[\text{HCO}_3^-]$, (C) $[\text{CO}_3^{2-}]$ and (D) pH. Data represent mean \pm sd.

Fig. 2. Exp. 2 Calcification response (measured as shell length) of *M. edulis* larvae kept under modified carbonate chemistry conditions for four days during the lecithotrophic phase. Shell length is plotted against seawater (A) $p\text{CO}_2$, (B) $[\text{HCO}_3^-]$, (C) $[\text{CO}_3^{2-}]$ and (D) pH. Data represent mean \pm sd.

Fig. 3. Exp. 3 Calcification response (measured as shell length) of *M. edulis* larvae kept under modified carbonate chemistry and C_T limiting conditions for four days during the lecithotrophic phase. Shell length is plotted against seawater (A) $p\text{CO}_2$, (B) $[\text{HCO}_3^-]$, (C) $[\text{CO}_3^{2-}]$ and (D) pH. Data represent mean \pm sd.

Fig. 4. Meta-analysis of the relative calcification response (as % of control): bivalve larvae during the lecithotrophic phase plotted against seawater $[\text{HCO}_3^-]/[\text{H}^+]$ (A) and Ω (B). Comparison of *Mytilus* spec. larvae and juveniles plotted against calculated seawater $[\text{HCO}_3^-]/[\text{H}^+]$ (C). Exp. 4 Shell length of *M. edulis* larvae 70 hpf plotted against seawater $[\text{HCO}_3^-]/[\text{H}^+]$ (D). Relative calcification rates were calculated from either shell length (larvae) or shell mass growth (juveniles).

Fig. 5. Changes of physiological rates during the ontogeny of *M. edulis*. (A) respiration and calcification rates during the planktonic larval phase. (B) absolute calcification rates of larvae and juveniles (nmol h^{-1}). (C) relative calcification rates ($\text{nmol h}^{-1}\text{mg}^{-1}$) of larvae and juveniles. Data represent mean \pm sd.

Fig 1

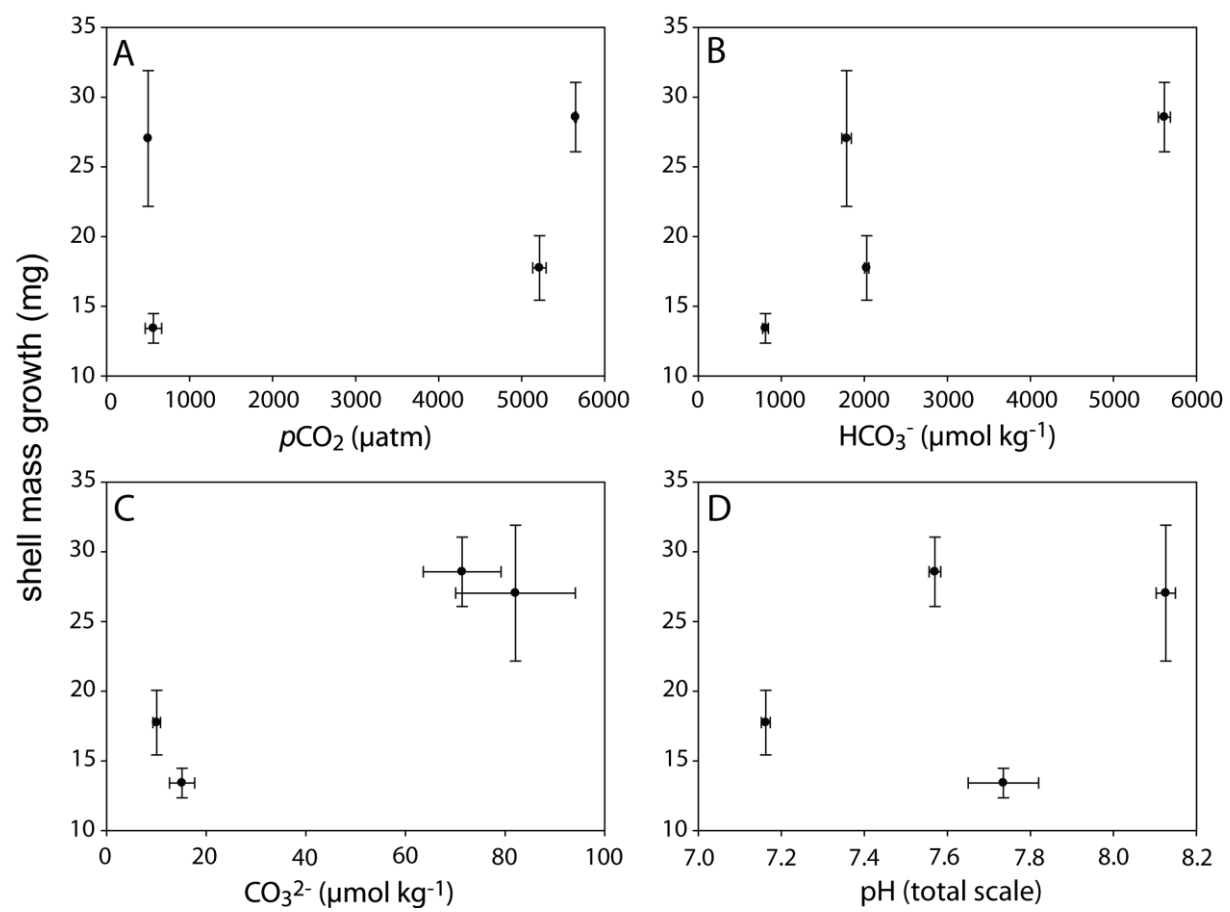


Fig. 2

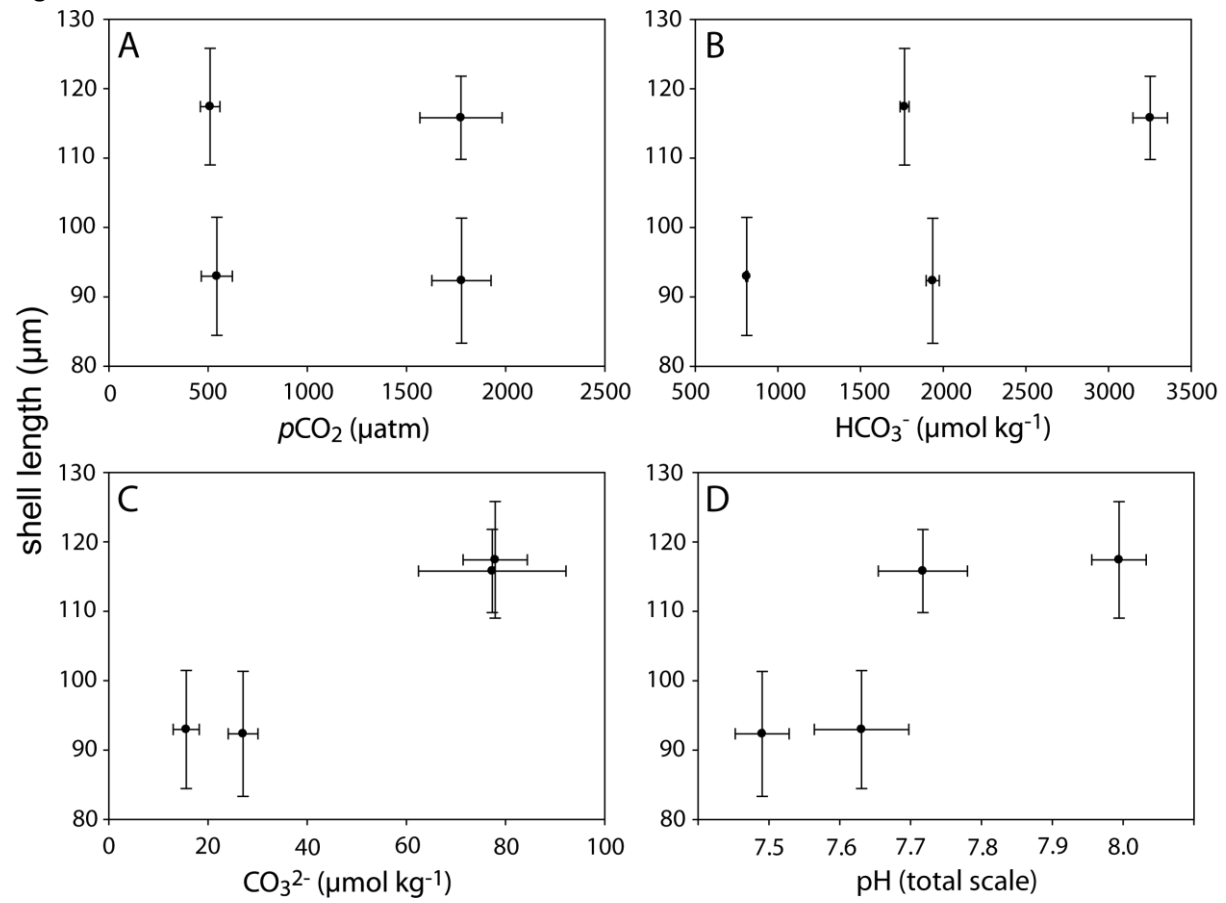


Fig.3

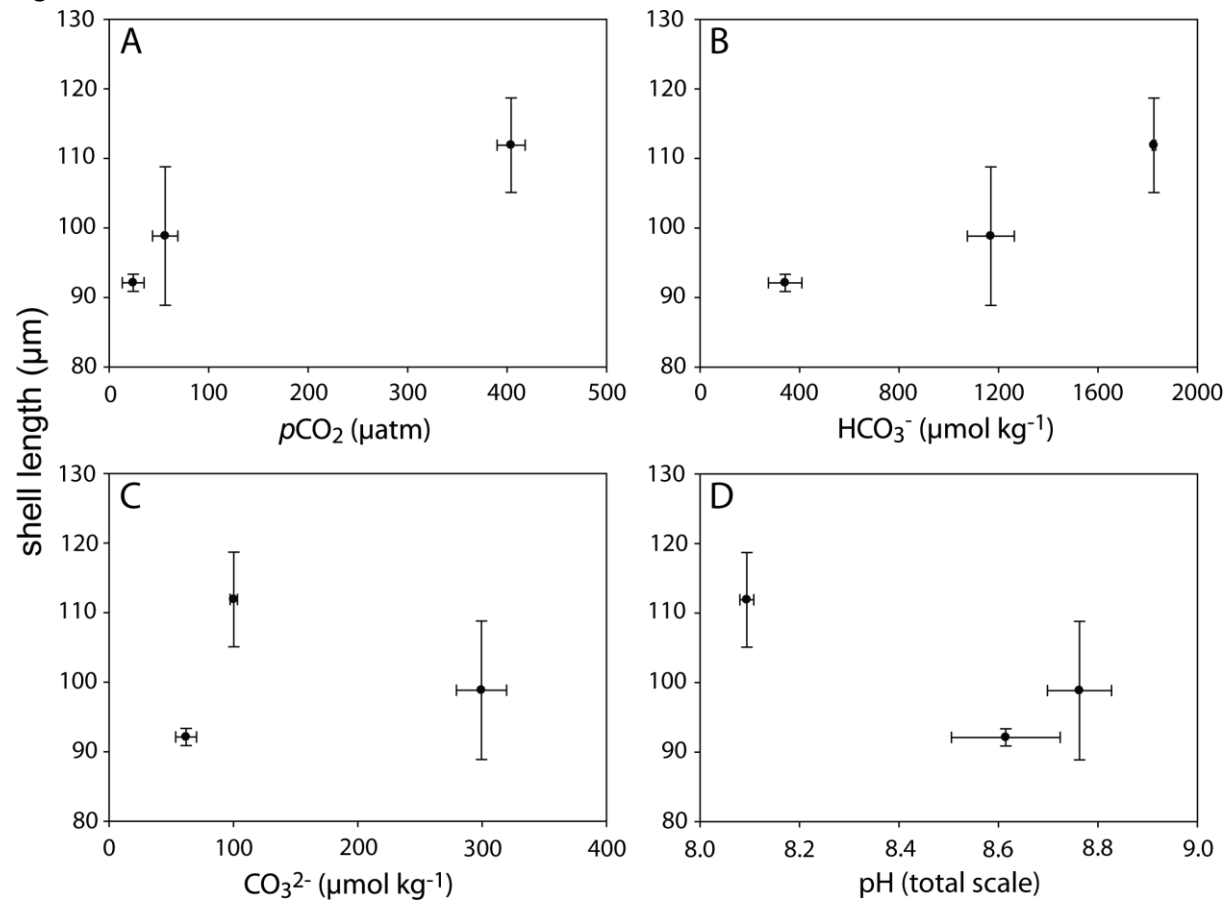


Fig. 4

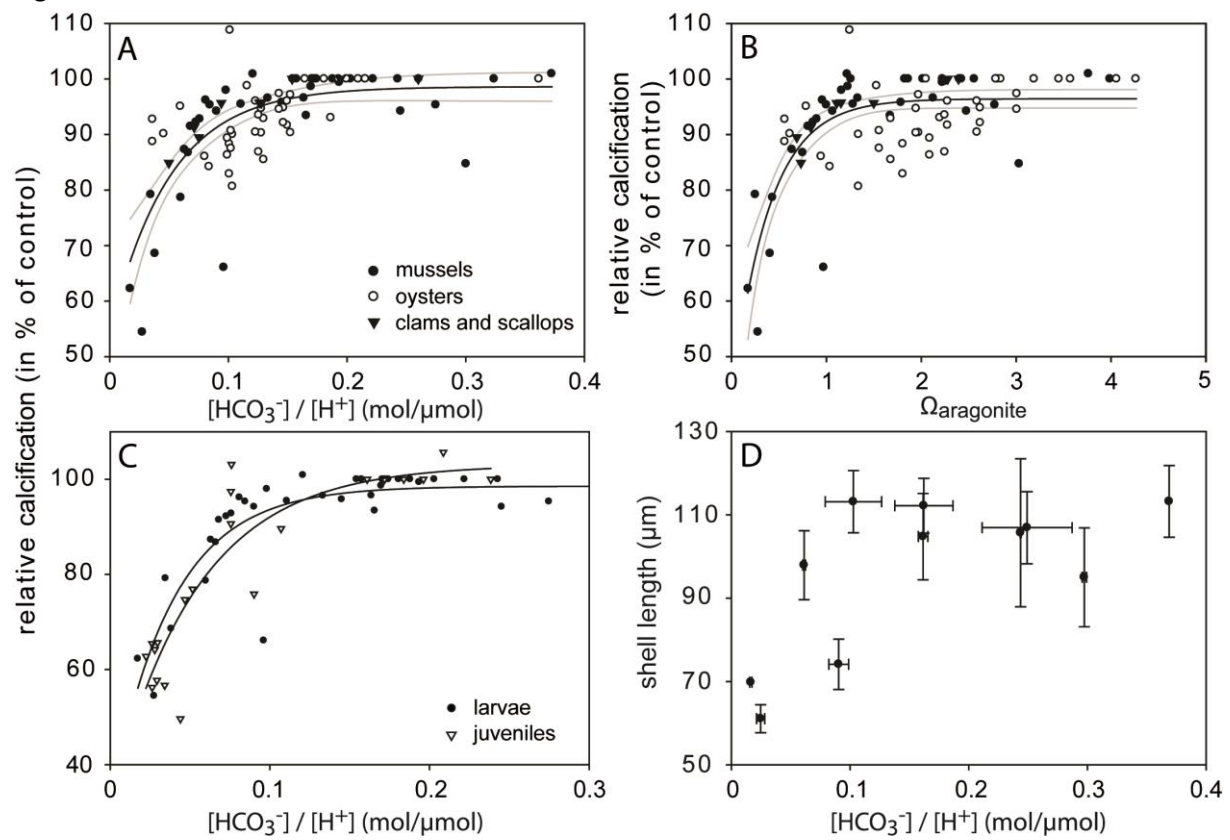


Fig 5

